CHALMERS
UNIVERSITY OF TECHNOLOGY

Effects of ASE noise and total injected power on Optical Injection Locking

Master's thesis in Electrical Engineering

MIGUEL RUIZ

Department of Microtechnology and Nanoscience
CHALMERS UNIVERSITY OF TECHNOLOGY
Gothenburg, Sweden 2019

Master's thesis 2019

Effects of ASE noise and total injected power on Optical Injection Locking

MIGUEL RUIZ

CHALMERS
UNIVERSITY OF TECHNOLOGY

Department of Microtechnology and Nanoscience
Photonics laboratory
Fiber optics group
Chalmers University of Technology
Gothenburg, Sweden 2019

Effects of ASE noise and total injected power on Optical Injection Locking
A Subtitle that can be Very Much Longer if Necessary
MIGUEL RUIZ

Supervisor: Ravikiran Kakarla, Photonics Laboratory, Department of Microtechnology and Nanoscience, Chalmers University of Technology, Gothenburg.
Examiner: Prof. Magnus Karlsson, Photonics Laboratory, Department of Microtechnology and Nanoscience, Chalmers University of Technology, Gothenburg.

Master's Thesis 2019:NN
Department of Microtechnology and Nanoscience
Photonics Laboratory
Fiber optics group
Chalmers University of Technology
SE-412 96 Gothenburg
Telephone +34 697383812

Cover: Wind visualization constructed in Matlab showing a surface of constant wind speed along with streamlines of the flow.

Typeset in LaTeX
Printed by [Name of printing company]
Gothenburg, Sweden 2019

Effects of ASE noise and total injected power on Optical Injection Locking
A Subtitle that can be Very Much Longer if Necessary
MIGUEL RUIZ
Department of Microtechnology and Nanoscience
Chalmers University of Technology

Abstract

Optical Injection Locking (OIL) phenomena has substantial importance in communications systems, making stable locking with low injected power a major challenge. Additional considerations involve that nature of oscillations in the lasers is random, provoked by temperature and spontaneous noise.
An OIL setup was constructed in order to get stable injection locking with the lowest input power from the master laser. Moreover, with the aim of improving this parameter, a phase locked loop (PLL) was developed. This addition requires the initial setup to include a modulator, that in this case works at 6 GHz. The modulation was verified, ensuring that side bands are distanced enough, preventing the slave laser from locking at unwanted frequency.
Previous studies show that there is an optimum input slave power that minimizes the phase noise. We measure the phase noise applying two type of power at the input, ASE noise and master laser power. The experiment aims to discover the parameter that limits the OIL, whether it is the total input power into the slave laser (keeping OSNR constant) or the master power. An appropriate topology was used to differentiate between the different sources of power. The main reason to design this experiment is advance in the understanding of the factors that influence OIL. To achieve this, we prepared two set of measurements tuning different parameters. The first test keeps ASE noise power constant while the master laser power is swept. For the second test, OSNR is fixed and total power is changed.
Comparing the resulting phase noise will provide knowledge on the behaviour of the locking bandwidth.

Keywords: OIL, PLL, ASE noise, laser, OSNR.

Acknowledgements

I would like to thank my mentors in this thesis, Ravikiran Kakarla for guiding me through this project, and Magnus Karlsson for proposing it and give me the chance to work in the photonics laboratory.

I cannot forget my professors in the fiber optics communicactions course, Jochen Schroëder and Peter Andreksson, who opened the doors of the group for anyone interested.

Of course, I will always be in debt with my parents and brother, who always trusted me.

Miguel Ruiz, Gothenburg,August 2019

Contents

List of Figures

List of Tables

1

Introduction

Clock synchronization has always been a major challenge in telecommunications. Distributed systems need to operate at the same clock frequency to avoid phase noise and other problems such as jitter and skew. In the case of not respecting this principle, we will experience a degradation in performance.
Laser synchronization can be understood as an appropriate analogy in the optical environment. OIL is the procedure where a free running laser (slave) is injected with light from another laser (master), making the slave to emit light with the same frequency and phase. Injection locking has numerous applications, such as phase sensitive amplifiers (PSA) [1], phase sensitive demodulation, synchronization of chaos and others [2,3,4,5].
In the work presented in [2], there is a major finding in the stabilization of laser's oscillation frequency. This method relies on a mechanism that permits the laser to self-lock at a resonance of a separate Fabry-Perot cavity. Futhermore, it is possible to reduce the laser linewidth. This unconventional geometry allows improved performance in applications such as OIL, optical feedback and electronic servo control.
Injection locking techniques will also have a huge impact in the new 5G standard. A wide range of band frequencies are allocated for the services that this technology will provide (30-90 GHz). High quality video on demand, autonomous vehicles and interactive multimedia entertainment would overcrowd the current spectrum. In order to avoid this, millimetre waves communication will be used, and optical fibers are a considered an interesting option. They provide wide bandwidth and low cost, which makes them appropriate for the transport of mm-wave signals. Thus, the frequency stability and phase noise of the carriers are a key factor in the overall performance of the system. Ref. 3 studies the stability of a distributed Bragg reflector laser (DBR) as a slaver laser when it is injected with different powers and wavelengths. The results show a maximum locking range of 172 MHz regardless how much we increase the injected power.
In the researches [4,5] is presented the result of performing OIL with vertical cavity surface emitting lasers (VCSELs). Ref. 4 shows that the frequency response of an injection locked VCSEL laser is similar to a parasitic limited laser with high resonance frequency.
For similar purposes, optical phase locked loops can be employed. However, the higher complexity when using semiconductor lasers makes it less popular. In some studies [6], these two techniques are combined with significant improvements in locking bandwidth and phase error.
In prior work to this research [1], it is measured phase noise has been measured for different slave input powers and OSNR's. However, it has not investigated the effect

of noise surrounding the master laser (ML). The thesis aims to solve the dilemma of the parameters that limit locking bandwidth, whether it is total power into the slave laser (SL) or ML power itself (for the same OSNR). To answer this question, it is essential to propose a setup that allows us to measure the different contributions to the slave laser. If the phase noise increased with total power (fixed OSNR), noise would affect even if master can be amplified. It is essential to know if there is a limit that contradicts this statement.
In addition to this, a PLL is added on the injection locking setup to improve the performance. Ref. 1 uses a 10 GHz modulator, which enhances the action of the PLL to record input power to -65 dBm. We aim to reach the same limit with a lower modulation (6 GHz), removing the necessity to use higher frequency signal generators.
From a a general point of view, it seems clear that new services that we cannot even imagine will be deployed in the next years. Many of them will require high amounts of bandwidth at mm-wave bands. This further underlines the value of fiber optic communications and the research on frequency stability of lasers. Actually, their importance is not restricted to the IT and communications sector. Investments of the medical industry are growing significantly. Transatlantic surgeries might be possible with the 5G network, that will provide a latency of 1 ms. Also, the entertainment sector will also be benefited by this feature, allowing real time, low latency communications between players all over the world.
5G will handle thousands of million of sensors connected 24/7, transmitting information about, temperature, humidity, quality of air, as well as data related to our daily habits. The processing of this information in big data centers must be efficient in order to avoid bottlenecks and obtain benefits from the data.
As a consequence of this, it is expected a raise in the economic activity worldwide, which should be equivalent to an improvement of life standards and welfare.
However, some challenges must be faced, like the proper functioning of pump recovery systems when input power is lower than -45 dBm (without PLL), causing a degradation in performance in phase sensitive amplifiers (PSA). The thesis is organized as follows. Chapter 2 includes all the concepts necessary to understand the topic. It consists of a brief review of OIL key parameters, laser theory, non linear effects and sources of noise. In chapter 3 is described the experiment setup and every component utilized, as well as its function and characteristics. In chapter 4 we comment the results obtained and its contribution to the state of the art. Finally, chapter 5 is a discussion where we show the conclusions of the research.

2

Theory

In this chapter is introduced all the theory needed to understand the experiment and interpret the results that will be commented in the final part. OIL phenomena is presented, as well as all the factors that characterize its behaviour and nature.

2.1 Single mode semiconductor lasers

Semiconductor lasers are widely used in optical links. With the ability of providing a complete range of wavelengths (400nm-2000nm) and high output powers, as well as constant, they have become the most popular option in many areas. Their operation is based on cavity loss, that is wavelength dependent and the main types are:

- Distributed feedback lasers (DFB) are the most common, which provide a wavelength selective grating in the cavity, besides being temperature tunable ($\sim$ 5 nm). They are proved to be the most stable and can provide high powers (kilowatts).
- External cavity lasers use a frequency selective element that is located outside the cavity. Its main strength is the high tunability ($\sim$ 50 nm).
- Vertical cavity surface emitting lasers (VCSEL) supply an output orthogonal to the substrate, in the same form that some LED works. This type of lasers appeared in the 90's and were adopted rapidly for a great number of applications. Only one longitudinal mode is used for the use of a very small cavity ($\sim 1\mu m$). The main limitation is the low power that can provide (in the order of few miliwatts).

From Maxwell equations we can deduce expressions that describe the behavior of semiconductor lasers, which are described by [16]:

$$\frac{dP}{dt} = GP + R_{SP} - \frac{P}{\tau_p} \tag{2.1}$$

$$\frac{dN}{dt} = \frac{I}{q} - \frac{N}{\tau_c} - GP \tag{2.2}$$

where N is the number of electrons, P is the number of photons, GP is the stimulated emission, R_{SP} is the spontaneous emission and τ_p is the photon loss rate, τ_c is the spontaneous emission and q is the electron charge. Eqn 2.1 and 2.2 explain the static and dynamic nature of semiconductor lasers.

2.2 Types of noise

In every source of light there are sources of unwanted signal that lead to fluctuations in gain and wavelength. Two main mechanisms of noise are the shot noise and thermal noise because they are present in every optical system.

2.2.1 Thermal noise

Every particle that has a non zero temperature suffers a thermal motion. This movement is proportional to the temperature and it can be expressed as [14]

$$\sigma_T^2 = 2 \int S_T(f) df \approx (4k_B T/R_L)\Delta f, \tag{2.3}$$

where k_B is the Boltzmann constant, T is the temperature, R_L is the load considered and Δf is the bandwidth. $S_T(f)$ is the noise spectral density.

2.2.2 Shot noise

Shot noise is related with the nature of how a current is generated. This generation is part of random of process (usually approximated by a Poisson process), what causes an uncertainty on the current. This contribution can be calculated with the following equation:

$$\sigma_S^2 = 2q(I_d + I_p)f, \tag{2.4}$$

where q is the charge of an electron, I_d is the dark current, I_p is the current from a laser or photodetector and Δf is the bandwidth considered.

2.2.3 Amplified spontaneous emission

All optical emitting components are based on the phenomena of absorption, stimulated emission and spontaneous emission. Figure 2.1 shows the band model where E_1 is the ground state and E_2 is the excited state. When the energy of an incident photon is higher than energy difference (E_2-E_1) it becomes part of an atom in the excited state. Eventually, the atom returns to ground state and it will emit light. This is the case of spontaneous emission, where photons are emitted with random phase and directions (Light emitting diodes). Stimulated emission starts with an existing photon interacting with an atom in the excited state. Resulting photons maintain the same energy, phase and direction of propagation.

2.2.4 Phase noise

The deviation of phase between SL and ML is called phase noise. Ideally, lasers emit at one single frequency, but in reality their spectrum has a width. This frequency fluctuations are translated into the time domain as phase shifts. Stability can be divided in two types [33]:

- Long-term stability - frequency shifts observed during several hours, days or months.

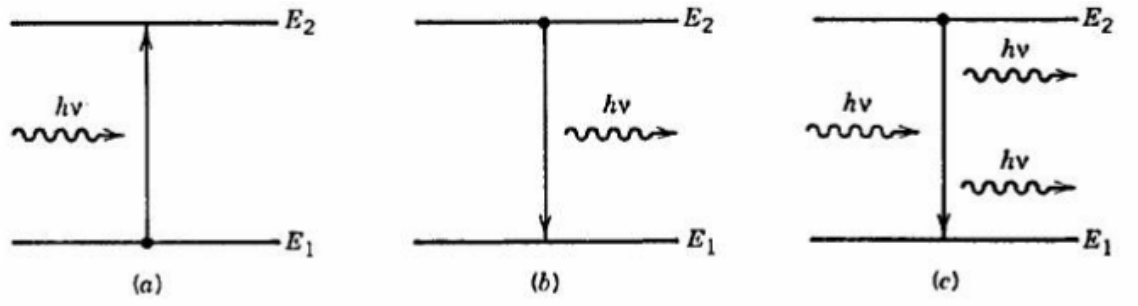

Figure 2.1: Representations of the absorption of a photon (a), spontaneous emission (b) and stimulated emission (c) [14]

- Short-term stability - frequency shifts observed during few seconds.

In this work we will focus on short-term stability, because this is the kind of disruptions that fit better the thermal drifts present in OIL. The nature of this phenomena is random, so behavior is explained properly with a spectral density function. With this information, we can get information of how probable a phase bias is.
One classic measurement is the single sideband phase noise(SSB), and it is denoted as L(f).

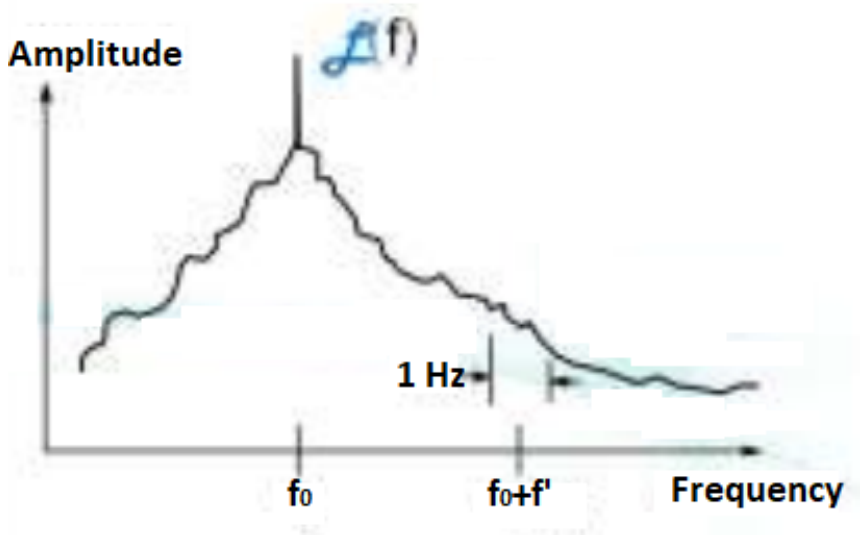

Figure 2.2: SSB expression in dBc/Hz, as well as spectral density function [32]

Figure 2.2 shows the plot of a single sideband phase noise within a 1 Hz of bandwidth at a f' frequency from the carrier. L(f) is given by [32]:

$$L(f) = \frac{Area\ under\ 1Hz\ bandwidth}{Area\ under\ the\ curve} \tag{2.5}$$

2.3 Non linear effects

One of the main applications of OIL is pump regeneration, which is employed in PSA amplifiers. In these systems, the transmitter is formed by a copier (HLNF)

to create an idler wave, that is the product of four wave mixing (FWM) from the pump and data signals. In the receiver side, the pump is separated from idler and data. OIL must amplify the pump signal with the lowest noise to obtain the highest possible gain. [1]
Nonlinearities are helpful to reach maximum benefits in areas of research where OIL is utilized. In nonlinear optics light cannot be studied as a superposition of sources of energy propagating because new frequencies can appear and interact between them. In addition to this, optic fibers are usually long, which enhances the accumulation of non linear effects and the core is small so electric field is confined in reduced size. The power launched into the fiber is the major factor for nonlinear behaviour. At low power levels effects are negligible and the BER in these cases is limited by noise, but there is a limit in the input power without assuming limitations. There are two types of non linear effects: [14]

- Electrostriction. Intense electric field cause changes in the shape and density of the medium. Thus, refractive index varies. It causes stimulated Brillouin Scattering (SBS), that scatters and downshifts light in the backward direction by 10 GHz.
- Kerr effect. Optical power change refractive index provoking self phase modulation (SPM), cross phase modulation (XPM) or four wave mixing (FWM). As a consequence of this, frequency downshifts ($\sim$ 13 THz) are created and they are known as stimulated Raman Scattering (SRS) [14]. By contrast with SBS, this phenomenon occurs in both the backward and forward directions.

2.3.1 Self phase modulation

Propagation constant depends on $\tilde{n}_2$, and the nonlinear-index coefficient are related following [15]

$$\beta' = \beta + k_0 \tilde{n}_2 P / A_{eff} \equiv \beta + \gamma P, \tag{2.6}$$

where A_{eff} is the effective mode area, β is the propagation constant and $\gamma = 2\pi\tilde{n}_2/(A_{eff}\lambda)$. This term produces a nonlinear phase shift expressed as [15]

$$\phi_{NL} = \int_0^L (\beta' - \beta) dz = \int_0^L P(z) dz = \gamma P_{in} L_{eff,} \tag{2.7}$$

where P(Z)=P_{in}exp(-α z) and L_{eff} is the effective length. This causes a self induced nonlinear phase shift, and also induces pulses to be chirped. Figure 2.3 shows how SPM does not affect the amplitude, but introduces a phase shift in the time domain. This leads to spectral broadening in the frequency domain.

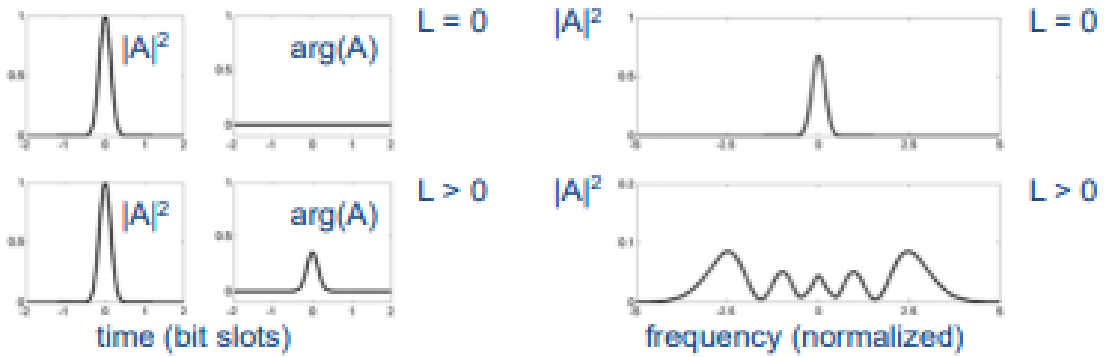

Figure 2.3: Effects of SPM in frequency domain [16]

2.3.2 Cross-phase modulation

When various wavelength channels of light are travelling through an optical fiber cable (WDM, wavelength division multiplexing) there is a nonlinear phase shift. But this is not only limited to the case explained previously (SPM), but the power of each channel affects the phase of other channels. Couplings between transmission lines in electrical boards (crosstalk) is a fair analogy in electrical systems. The phase shift for the j^{th} channel is [15]

$$\phi_j^{NL} = \gamma L_{eff} \left(P_j + 2 \sum_{m \neq j} P_m \right), \tag{2.8}$$

where P_j is the power in each channel and L_{eff} s the effective length. We can observe that XPM doubles (factor 2) the repercussions of SPM. Nevertheless, the pulses have to be transmitted in the same period time to be mutually affected. Changing the phase can give a rise to a chirp that causes a translation in frequency domain (up or down).

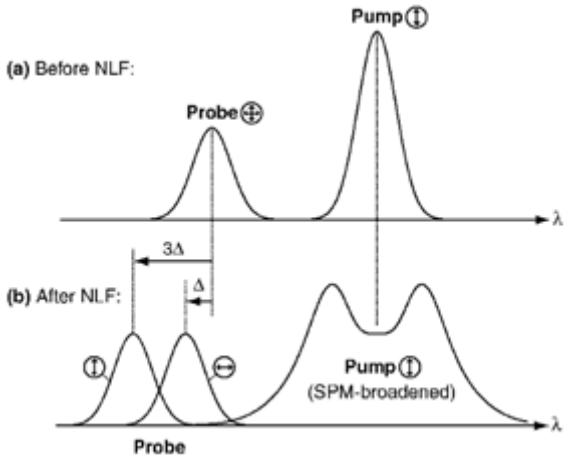

Figure 2.4: Effects of XPM in time and frequency domain [17]

Another drawback is that XPM introduces timing jitter, due to the frequency shift

and dispersion.[18]
SPM and XPM cause the modulation of phase wave with itself or other waves respectively, but there is not any new frequency component.

2.3.3 Four-wave mixing

Previous nonlinear effects shown in this chapter present the appearance of spectral broadening, frequency shift, or soliton pulses. FWM involves the generation of a new mode propagating. If three wavelengths travel through a fiber, an additional one is generated at a frequency $\omega_4 = \omega_1 \pm \omega_2 \pm \omega_3$ [17]. In general, for N frequencies, $\frac{N^2(N-1)}{2}$ products from FWM are obtained. All these spectral components are rarely generated in reality due to mismatch in phases.
The most conflictive combination is usually $\omega_4 = \omega_1 + \omega_2 - \omega_3$ because they combine in phase when channel is on zero dispersion wavelength. Moreover, in equally spaced channels FWM products can overlap the pulse.

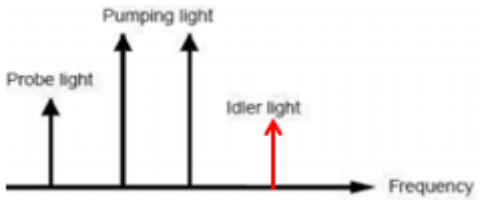

Figure 2.5: Effects of FWM in frequency domain [18]

2.4 State of polarization (SOP) of light

Taking control of light polarization is a fundamental aspect in many optical applications, and OIL is not an exception. For an appropriate locking, ML SOP must match the state of the SL [17]. Light is said to be unpolarized if the direction of electric field vibrates randomly. By contrast, when fluctuations are deterministic, light is said to be polarized [18].
The main types of polarization are:

- Linear: every fluctuation of the electric field can be confined inside a plain along with the direction of light.
- Circular: Electric field rotates around the direction of propagation forming a circle. It has two components with the same amplitude and a phase difference $\pi/2$.
- Elliptic: Electric field rotates around the direction of propagation shaping an ellypse. Vector components do not have to maintain equal amplitudes or phase difference is not $\pi/2$.

A second classification can be made according to the sense of rotation. If it is clockwise, wave is said to be right circularly polarized. In the other hand, if rotation is counter clockwise the light is left circularly polarized.

The wave corresponding to the electric field associated to a beam of light must have the following form (solution to Maxwell's equation):

$$\mathbf{E}(\mathbf{r},t) = \mathbf{E}_0 e^{i(\mathbf{kr}-\omega t)} \tag{2.9}$$

where $\mathbf{k}$ includes the direction of propagation. In isotropic medium it is known that $\mathbf{E}_0$ and $\mathbf{k}$ is perpendicular, but even though $\mathbf{k}$ is perfectly known, the exact direction of $\mathbf{E}_0$ cannot be stated. To solve this issue, we will overlap z axis with $\mathbf{k}$, thus (2.9) can be written as [19];

$$\mathbf{E}(z,t) = (E_x\mathbf{x} + E_y\mathbf{y})e^{i(kz-\omega t)} \tag{2.10}$$

where E_x and E_y are the amplitude of the electric field in dimensions x and y respectively. From these values we can get to know the SOP of the wave. In the case of any of these magnitudes were null, the light is linearly polarized. The same happened for equal or π phase shift.

2.5 Jones calculus

In 1941 Jones developed a notation to describe fully polarized light [19].The Jones vector represents polarized light, whereas Jones matrices represents linear optical elements [20].
This calculus is correct in the case of polarized light in free space and isotropic non attenuating medium, where a transverse wave is a good model for light. We always orient the propagating light towards the z axis, and using equation (2.10), we can express the Jones vector as [19]

$$E_J = \begin{pmatrix} E_{0x}e^{i\phi_x} \\ E_{0y}e^{i\phi_y} \end{pmatrix}, \tag{2.11}$$

where we get information about magnitude and phase of the electric field. Ina addition to this, it can be necessary to obtain polarization states after optical elements, like polarizers and wave plates at arbitrary angles. This situation is obtained with this expression [19]

$$E_{OUT} = J_{system}E_J, \tag{2.12}$$

where J_{system} is the Jones matrix, obtained from the matrixes of all the optical elements (N).

$$J_{system} = J_N J_{N-1}...J_1 \tag{2.13}$$

$$E_{OUT} = J_{system}E_J \tag{2.14}$$

2.6 Polarizers

These are the elements used to polarize light. Some of the most common are [22]:

- Reflective: light reflects differently the distintict polarizations, conserving only one of them.
- Dichroic: unwanted polarizations are abosrbed, taking advantage of materials that present the feature of anisotropy.
- Birefringent: light is divided due to refraction when it incides on a crystal.

Polarizers have some key features that are useful to characterize their performance.

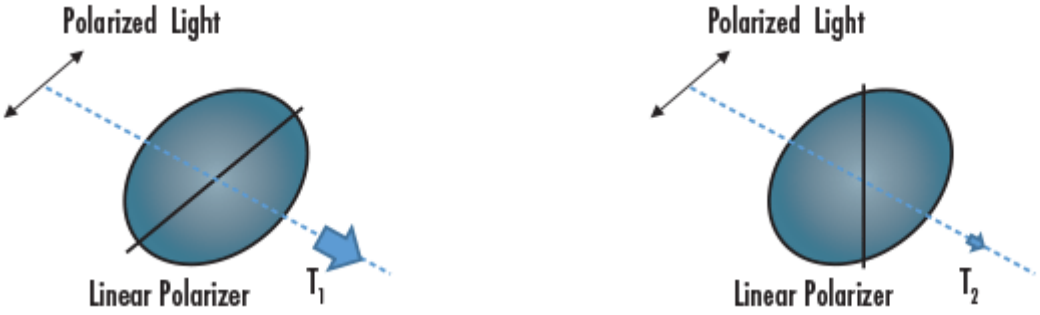

Figure 2.6: Scheme of the representation of T_1 and T_2 parameters [21]

Figure 2.6 shows the main factors to characterize a polarizer. T_1 represents the maximum power transmitted when polarization axis is the same than polarized light. On the other hand, T_2 is the minimum power when transmission axis is perpendicular to polarized input light.
From this, the degree of polarization, P, and extinction ratio are defined, ρ_p with the following expressions [21]:

$$P = \frac{T_1 - T_2}{T_1 + T_2} \tag{2.15}$$

$$\rho_p = \frac{T_1}{T_2} \tag{2.16}$$

Low cost polarizers are in the range of 100:1, whereas high performance birefringent polarizers can reach a value of 10^6.

2.7 Optical Injection Locking

Injection locking (IL) has been documented in early times in history. In XVII century Christian Huygens already described this phenomena in a letter sent to his father [7]. Basically, he states how the clocks on a wall tend to synchronize (initially not synchronized), involving that they maintain the same phase and frequency. He reached the conclusion that time required to synchronize depended on the distance between them, and steady state was a product of vibrations.
More recent studies have been carried out, advancing from electrical to optical systems. In 1946 Adler concluded that frequency difference between two oscillators if locking wants to be achieved [8]. Later extensions brought the first optical injection locking experiment, when Stover and Steier were able to lock two He-Ne lasers [9]. The process of cloning one laser, known as master laser (ML) with another (slave laser, SL), transferring the properties of phase and frequency depends on the locking bandwidth, a parameter that relays on the ratio of powers between lasers. There is always a frequency gap between ML and SL, $\Delta\nu = \nu_{ML} - \nu_{SL}$. This gap must be inside a certain limit to make OIL possible, and this range is known as the locking bandwidth. It can be expressed as [10]

$$\Delta\omega_{LB} = \sqrt{1+\alpha^2} f_d \sqrt{\frac{P_{inj}}{P_{sl}}}, \tag{2.17}$$

where α is the linewidth enhancement factor (typically around 5 [4]) and f_d is longitudinal mode spacing. P_{inj} and P_{sl} are the power injected to the SL and the free running laser output respectively. The ratio of these magnitudes form the Injection ratio (IR), which is a key parameter in the OIL process, i.e.

$$IR = \frac{P_{inj}}{P_{sl}}. \tag{2.18}$$

It is well known that all lasers have a certain linewidth due to noise from spontaneous emission. In addition to this, carrier density affects the refractive index and optical gain, creating a phase amplitude coupling. Experimentally, the factor that approximates in a more accurate way the effect of linewidth widening is $\sqrt{1+\alpha^2}$ [11].The parameter α links phase and gain proportionally [12]

$$\Delta\phi = (\alpha/2)\Delta g, \tag{2.19}$$

which also makes a laser to emit a chirp when working on continous wave mode. As we will see in the experimental part, a free running laser behavior drift up to 80 MHz (DFB laser, EM4, 1550 nm,17 dBm output power) , which means that locking bandwidth should be higher to achieve injection locking. Without the assistance of a PLL, this can be done with an input slave power of -45 dBm. Below this value, unstability appears. The detuning frequency of ML and SL that can be rectified to maintain locking is proportional to the IR. It is remarkable that there is a broad unstable area inside the LB named injection locking induced pulsations (ILIP). The stable region is narrow, so it is essential that ML and SL show constant frequency over time.

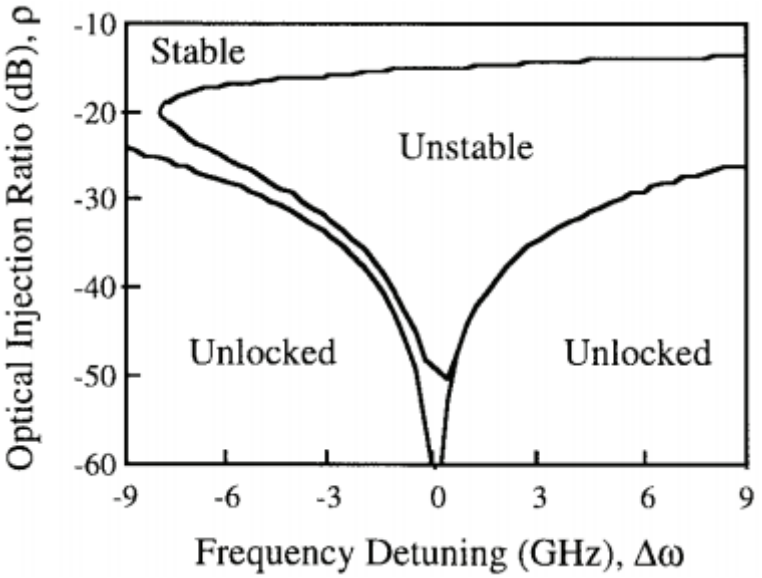

Figure 2.7: Locking regions for distincts IR and detuning frequencies [13]

Once the SL is locked (steady state), there is always a phase shift due to the frequency gap, given by [1]:

$$\Delta\phi = -sin^{-1}\left(\frac{\omega_{ml} - \omega_{sl}}{\Delta\omega_{LB}}\right) - tan^{-1}\alpha, \tag{2.20}$$

where $\omega_{ml} - \omega_{sl}$ are the frequency difference between ML and SL, $\Delta\omega_{LB}$ is the locking bandwidth and α is the linewidth enhancement factor. From Eqn 2.4 it can be stated that an increase in the locking bandwidth makes the phase shift lower. The PLL is introduced with the aim of compensating the appearance of frequency detuning due to thermal drifts and other sources of noise. The base of its operation is based on obtaining the phase difference between the SL and ML. To make this possible, a photodetector is used at the output of the injection locking setup to beat the fundamental tone (slave phase) with the side tones (master's phase). After translating the result to base band with a mixer, this signal is used as a modulation for the laser current driver in order to correct frequency deviations.

3

Experiment

In this section is described the setup employed on the implementation of the OIL and PLL. Moreover, we aim to show the functionality of all the components used in the process, as well as the additional setup utilized to measure all the experiments involved.

3.1 Setup scheme

Figure 3.1 shows a typical scheme to achieve OIL. We use a reflection style scheme, where only one facet of the light is used for coupling. By contrast, there is another way of performing IL. A transmission style scheme can also be implemented, where various facets are used for coupling. Reflection style was considered a better option due to the simplicity of the coupling.

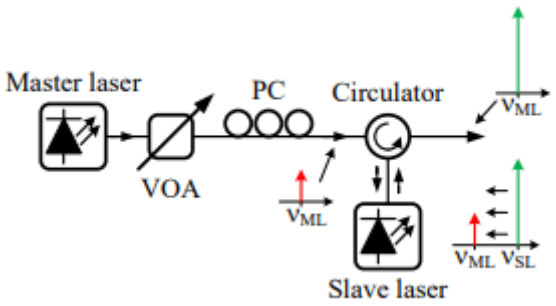

Figure 3.1: Schematic scheme of the experiment. VOA, variable optical atenuator; PC, polarizer controller.

The circulator couples the power from ML to the SL and isolates the SL to the ML, avoiding that there is not any reflected power. As we will see in the results part, there is a part of reflections that limit the performance.
The SOP is controlled with the polarization controller. With this component we ensure that only light polarized through one direction goes through the circulator and thus the SL. The main advantage of this is that we have a constant input power into the laser and fluctuations are reduced.
The VOA is a key component that allows us to tune the input power into the laser, helping us to characterize the behaviour of the OIL setup.

Feedback is needed when the PLL is used, which adds complexity to the design, but enhances the locking capacity at low IR's. Figure 3.2 shows the full OIL setup.

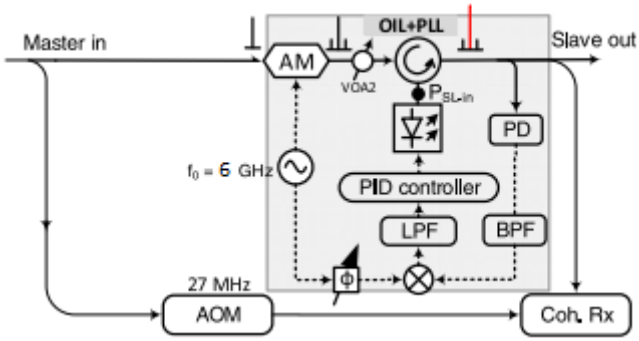

Figure 3.2: Setup of IL and PLL. AM, amplitude modulator; LPF, low pass filter; PD, photodetector; BPF,band pass filter; LO, local oscillator; AOM, acousto-optic modulator;PID, proportional integrator differentiator

The master laser (NKT photonics, 100 Hz linewidth) is modulated with 6 GHz modulator. This frequency is enough gap (higher than locking bandwidth) between the main and side tones. This process is useful to avoid that SL locks at unwanted side tones. The power from ML is coupled to the SL through a circulator. As it was indicated previously, the polarizer and the VOA permits a tuning of SOP and input power. At the slave output, there is a locked carrier with the slave phase, whereas the side tones have the master phase. This phase shift is used to drive the SL's current driver. PD beats the tones and a phase difference is obtained. The BPF reduces spectral noise and the mixer downconverts all the information to the base band. Afterwards, a LPF reduces noise and the PID controller converts phase difference in a modulating signal that will control the laser current driver.
With the aim of checking if the system is locked, IL output is connected to a coherent receiver, as well as the ML output, shifted 27 MHz after going through the AOM. For a locked situation, in the electrical spectrum should be present a tone at 27 MHz only.
We should note that this is the basic setup that inspires the real experiment carried out. However, the real scheme in the laboratory is more complex, because power and spectrum measurements have to be taken at the same time that OIL is performed. The additional components must be characterized too in order to know the error that they can introduce.

3.2 Laboratory setup

The main addition to Fig. 3.2 are the couplers, ESA (electrical spectrum analyzer), OSA (Optical Spectrum Analyzer) and the power metres. The ESA target is show the modulator output to check that a clean and stable carrier is generated at 6 GHz and tones are outside the locking bandwidth. For the OSA, temperature and current have to be tuned to move the SL wavelength into the ML center wavelength and maintain a locked state.

Table 3.1: Information of all the instrument utilized during the measurement process

Reference	Manufacturer	Name	Function
[23]	FS	FOPM-101	Power meter
[24]	Keysight	N9010A	Signal analyzer
[25]	ANDO	AQ6317	OSA
[26]	Agilent	8563E	ESA

Figure 3.3 shows all the components used in the laboratory for IL.

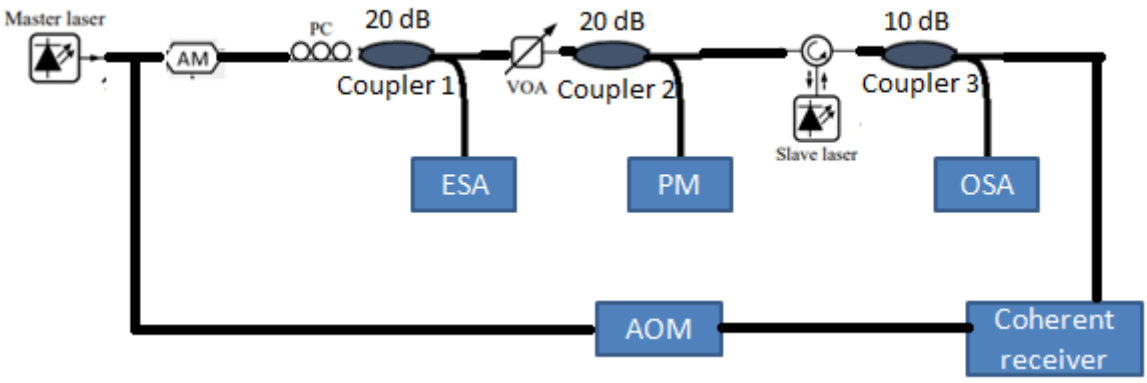

Figure 3.3: Detailed setup implemented in the laboratory. PM, power meter

Firstly, to make the whole system work we have to ensure that modulation step is done correctly. For this, the photodetector output is amplified and visualized in an ESA. Spectrum should show a strong carrier at 6 GHz and weaker side bands in DC and 12 GHz. This frequency gap is enough to avoid that locking mechanism degrades with interference with harmonics.
After that, we have to reach a steady state in injection locking phenomena. This is accomplished through the following steps:

- Tune the free running laser as near as possible to the wavelength of the ML (1554 nm). Temperature has a higher impact than current on the laser wavelength. Minimum temperature specifications (8-9ºC) are also a constraint for the wavelength tuning.
- A second tuning is performed to translate the free running laser to 27 MHz in the signal analyzer. Fluctuations are observed, but these should not be higher than 100 MHz (typical thermal drifts). Values of current and temperature are I=192 mA, T=10ºC.
- Raise the slave input power until both lasers are locked.

Table 3.1 presents all the components utilized throughout this projects, as well as the exact model.

3.3 Principal components

In this section is presented a brief description of the components that form the setup, such as the SL, circulator, photodetector, modulator and PID integrator.

3.3.1 Slave laser

The slave laser is an EM4, 50 kHz linewidth DFB laser.It is a CW InGaAsP/InP multi-quantum well (MQW) laser diode, ideal for high power applications and requirements of maintenance of polarization. This is the reason why all the fibers and components involved in the design are polarization maintaining.
In order to ensure steady state, temperature and current have to be tuned in order to set the output wavelength at 1554 nm (ML wavelength). The only available laser with the closest ML wavelength had its central frequency in 193.3 THz (1552 nm). The following values set the appropriate output wavelength (T=10ºC, I=192 mA).

3.3.2 Circulator

A circulator is a non reciprocal component, whose functioning is based on transmitting power from one port to the next one only. It has usually 3 ports and it is a passive element. Also, It is relevant that all devices introduce the minimum possible loss to reduce the error and obtain significant values of power into the SL.

Table 3.2: Specifications of the polarization maintaining circulator CIR-PM-15 [27]

Parameter	Values	
Center wavelength (nm)	1310±30	1500 ± 30
Insertion loss	0.9	
Peak isolation	50	
Typical isolation	46	
Min. isolation @23ºC	38	
Maximum power	300 mW	

It is important that reflections in port 2 of the circulator (connected to SL) are as low as possible. This can provoke a degradation of locking bandwidth mechanism if there is noise inside the locking range.

3.3.3 Photodetector

The photodetector is the device in charge of converting optical power into electric current. The magnitude that quantifies the amount of current generated for a given optical power is the responsitivity. The phase difference is obtained by beating the carrier (SL phase) and side tones (ML phase), which will be downconverted in the mixer.

The PD employed in the design presents a linear frequency response for high power applications (+15 dBm), which reduces the number of amplifiers. High performance in phase is also required.

Table 3.3: Specifications of the photodetector XPDV2120R [28]

Parameter	Values
Center wavelength	1480-1620 nm
Maximum avg optical input power	16 dBm
DC Responsitivity	0.65 A/W
Return loss	27 dB
Dark current	200 nA
3 dB cut-off frequency	50 GHz

The return loss of the photodetector is an important parameter because reflected power into the port 3 of the circulator (connected to the PD) can be transmitted to the ML, causing damages, as well as instabilities in the light into the SL.

3.3.4 Modulator

The Mach Zehnder scheme is one of the most widely used configuration for an amplitude modulator. In this work, a 6 GHz modulation is carried out to prevent side bands from disturbing OIL mechanism. A MZM is made of two phase modulators (one is enough) that shift this parameter, resulting in a constructive or destructive interference after output coupler

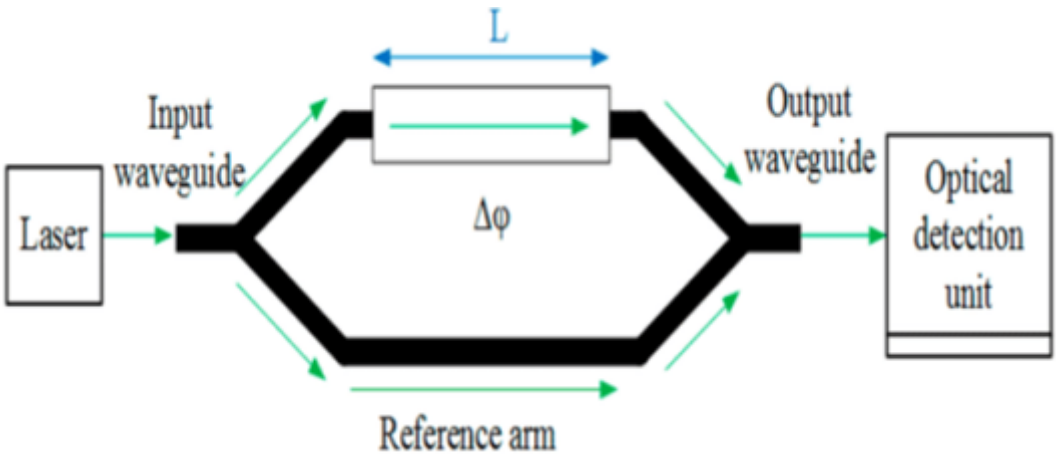

Figure 3.4: Block diagram of a Mach-Zender modulator [19]

The input waveguide is split in two paths (Figure 3.4). One of them will remain unchanged and works as the reference path, on the other arm light experiences a phase shift ($\Delta\phi$)after applying a voltage. The combination of these waves gives us a new one with a different amplitude, that depends on the phase shift applied.
A correct bias of the modulator is essential to make PLL work. A voltage sweep

is done checking the output power in order to know the V_π parameter of the modulator. The maximum output swing is reached by changing V_π from zero to 3.5V. Experimentally, we can state that $V_\pi = 3.5V$. Thus, an appropriate bias point for voltage is $V_b = -V_\pi/2$.
In this project is used a Lithium Niobate 10 Gb/s modulator, that present a long term bias stability, low modulation voltages and angled interfaces for minimal reflections.

Table 3.4: Specifications of the MZM 2623Y [28]

Parameter	Values
Operating wavelength	1525-1620 nm
Extinction ratio @DC	27 dB (typ)
V_{pi}	3.5 V
Dark current	200 nA
Return loss @6 GHz	-12 dB (max)
Dark current	200 nA
3 dB cut-off frequency	50 GHz

3.3.5 Couplers

In order to get accurate measurements is necessary to know the power that is being injected in the key parts of the setup, in this case is the SL. Couplers offer the possibility to split 1 input into 2 or more outputs, as well as the opposite operation (combining 2 inputs into 1 output).
Splitting 1 optical path into 2 allow us to use one of the ends to measure power and get to know the power circulating through the other path. To do so, a stage of characterization is needed to calculate the exact coupling factors of each divider. Table 3.5 shows the results obtained for each of the couplers:

Table 3.5: Coupling factors of all the couplers involved. These are numbered according to figure 3.3

Component	Coupling factor(dB)
Coupler 1	19.72
Coupler 2	20.99
Coupler 3	9.77

It is remarkable that coupler 2 (measuring P_{SLin}) suffers the highest bias (almost 1 dB) respect to the expected value, which confirms the necessity of characterization.

3.3.6 Mixer

The process of downconversion of the phase noise to baseband is done with a mixer. This is a non linear component with 3 ports, two of them are for the input signals. At the output is obtained the mixing of the frequencies of the signal in the form of:

- The sum of the frequencies.
- The substraction of frequencies.
- The original frequencies and its harmonics.
- Unwanted products of mixing ($2\omega_1$ $+\omega_2$, $2\omega_2$-ω_1,...).

The mathematical expression that describes the signal obtained at the output follows this expression:

$$V_s(t) = A_s x(t) cos(\omega_s t + \phi(t)) \tag{3.1}$$

$$V_o(t) = A_o cos(\omega_o t) \tag{3.2}$$

Multiplying with the use of a nonlinear component (diode), we can get this result:

$$V_s(t)V_o(t) = \frac{A_s A_o}{2} x(t)[cos(\omega_s - \omega_o t + \phi(t)) + cos(\omega_s + \omega_o t + \phi(t)) \tag{3.3}$$

In this case, we only use the difference of frequencies, so the other part of the spectrum is discarded.
The mixer was chosen because it fulfilled the required specifications of LO and mixing frequency, as well as a good performance on limiting the power couplings between the ports of the component (LO, Local Oscillator; RF, Radiofrequency; IF,Intermediate frequency).

Table 3.6: Specifications of the mixer used in the design (typical values)

Component	Value
IF max. frequency 1	4 GHz
Convertion loss	6.2 dB
LO to RF isolation	35 dB
LO to IF isolation	30 dB
1 dB compression point	4 dBm
1 dB compression point	4 dBm
LO input power	13 dBm (max)

3.4 Description of tests

In the work presented in Ref. [1] is shown a strong influence on phase noise due to IR and SL linewidth. Smaller linewidths reduce the frequency drifts and permit IL at low input powers. With the target of studying the limits of OIL, a combined input of ASE noise and power from ML is applied to the SL. From this point, they conclude that there exist an optimum P_{SLin} that minimizes phase noise. Basically,

laser linewidth limits OIL by causing phase noise for lower injection ratios.

The main problem is that we do not know the fraction of power into the SL that is ASE noise (P_{ASE})or ML power (P_{ML}). In this thesis is proposed an additional setup to the one presented in Fig 3.3, that allow us to have knowledge on P_{ML}, OSNR and P_{ASE}.
The discovery of which parameter decides the locking bandwidth, whether it is the ML power, or total power into the SL is based on two tests:

- Test 1: Sweeping P_{ML} for a varying OSNR and ASE power constant. We will obtain the phase noise for different OSNR and ML power onto the SL.

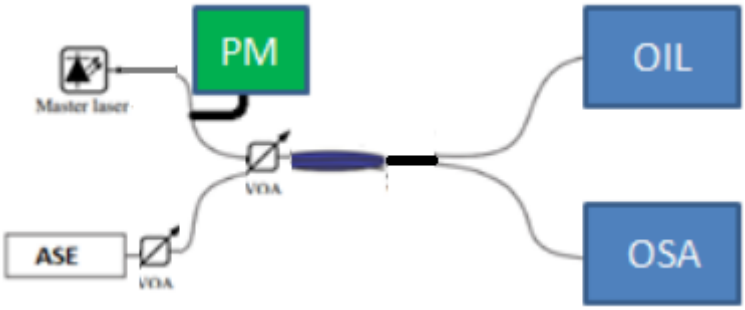

Figure 3.5: Topology to measure the basic parameters for the second test. PM, power meter; OIL, Optical Injection Locking setup; OSA, Optical Spectrum Analyzer

- Test 2: While the OSNR is fixed, we sweep the total power (P_{ASE} added to P_{ML}).

4

Results

Results from the OIL setup are presented in this chapter, showing the various levels of phase noise for distinct combinations of P_{ML}, P_{SL} and OSNR. It is common that input power to the slave laser is affected by noise (ASE noise). It is important to understand which factor limits the locking range, whether it is the total injected power or master laser power itself. In order to discover this, results from test 1 and test 2 will be compared. Test 1 sweeps P_{ML} for a fixed P_{ASE} for different values of OSNR, whereas test 2 sweeps total injected power for a fixed OSNR.
As shown in Eqn. 2.4, from phase noise we can deduce the level of locking bandwidth. It is remembered that a decrease in locking bandwidth involves an increase in phase noise and viceversa.

4.1 Measuring phase noise. Test 1

An OSNR sweep from 0 to 30 dBm was conducted for different values of ML power. Phase noise spectrum is ranging from 100 Hz to 1 MHz, it is shown the output SL power is 17 dBm. Respect to the signal analyzer, the power is integrated over a bandwidth of 1 Hz. We show single side band (SSB), phase noise (dBc/Hz). In figure 4.1 we can see the phase noise spectrum (FFT was performed). From 100 Hz to 2 kHz the measurement is not stable due to path vibrations and reflections in the circulator. The range 2 KHz to 1 MHz show a stable behaviour, with little fluctuations due to thermal drifts.

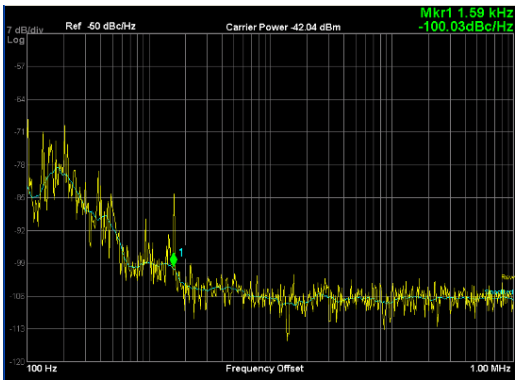

Figure 4.1: SSB phase noise spectrum for a ML power = -23 dBm

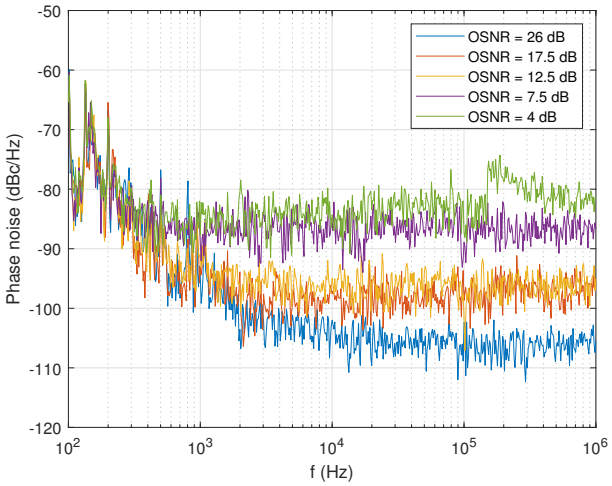

Figure 4.2: SSB phase noise spectrum in dBc/Hz for P_{ML}=-23 dBm. Frequency axis is in logarithmic scale

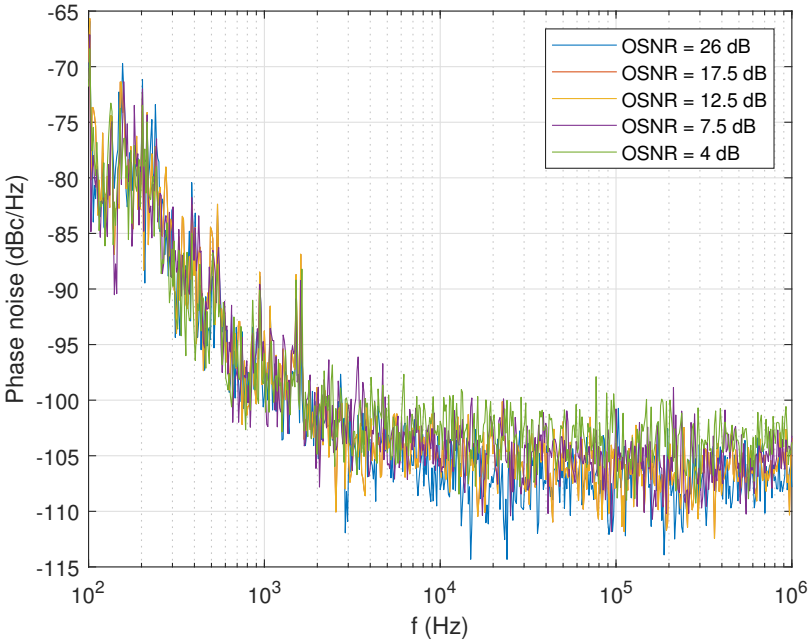

Figure 4.3: SSB phase noise spectrum for different OSNR's and ML power = -17 dBm

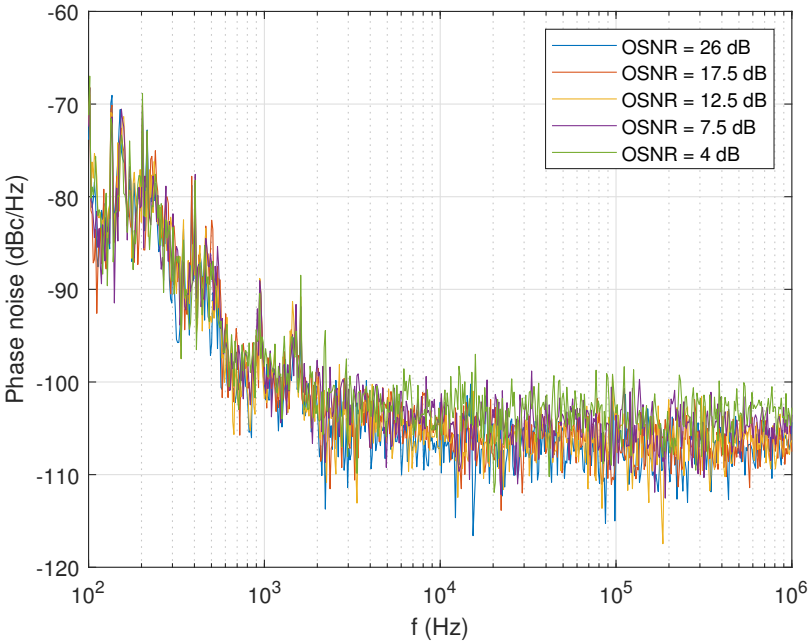

Figure 4.4: SSB phase noise spectrum for different OSNR's (dB) and ML power = -12 dBm

Figures 4.2-4.4 illustrate how OSNR degrades the locking bandwidth in OIL by increasing the level of phase noise.
When $P_{ML} = -23$ dBm (fig. 4.1) we can see clearly that a drop in OSNR have dramatic repercussions in SSB phase noise, whereas for higher P_{ML} powers (fig. 4.2-4.3) the OSNR has a lower impact. It is remarkable the decrease in phase noise at 200 KHz approximately for OSNR = 4dB (fig 4.1), increasing significantly the mean value of this parameter.

Also, it is interesting to analyze the values of the phase noise for different P_{ML} simultaneously in the same graph. This is shown in figures 4.5-4.6. The phase noise spectrum was integrated in all the frequency range measured (100 Hz - 1 MHz) in order to have an idea of the phase noise level under each input power. This integration was carried out using the trapezoidal method, so the value is approximated. However, the interval taken to make the calculations is only 1 Hz, that is the interval considered with the signal analyzer.

As expected, the phase noise for the lowest value of ML power involves a drop in locking bandwidth. Data is represented in two different figures because the phase noise P_{ML} = -23 dBm is an order of magnitude higher than for the rest of points considered. This means that there is a border in OIL performance when ML power is lower than -17 dBm, regardless of the OSNR.
Locking bandwidth drop due to noise raise can be explained from Eqn. (2.4). In locked state, SL suffers a frequency drift from any frequency gap between master and laser, as well as locking bandwidth (that depends on IR). These variations can be caused by thermal drifts, but this is not the case because then, variations would be the same for all the input powers. The real reason is the frequency variations due to linewidths in ML laser [2].

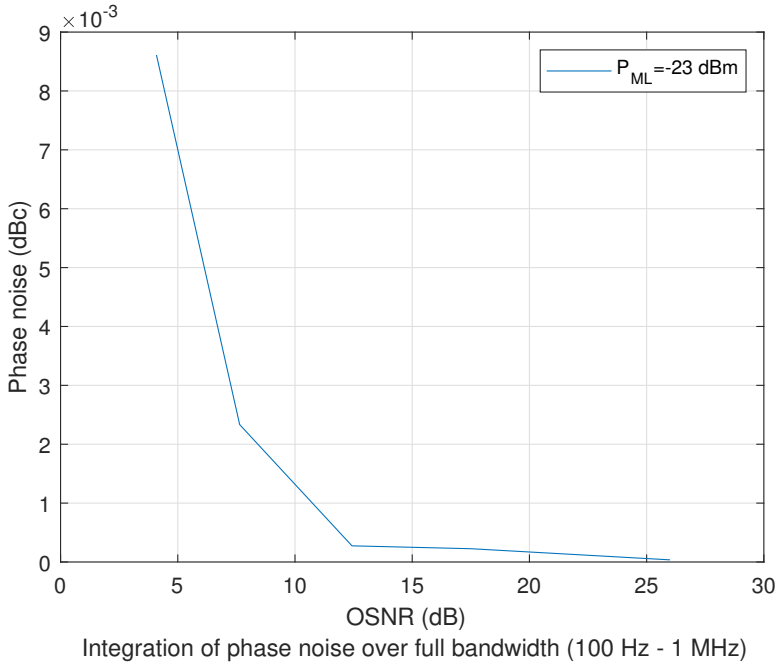

Figure 4.5: Integration of SSB phase noise spectrum for different OSNR's and ML power of -23 dBm

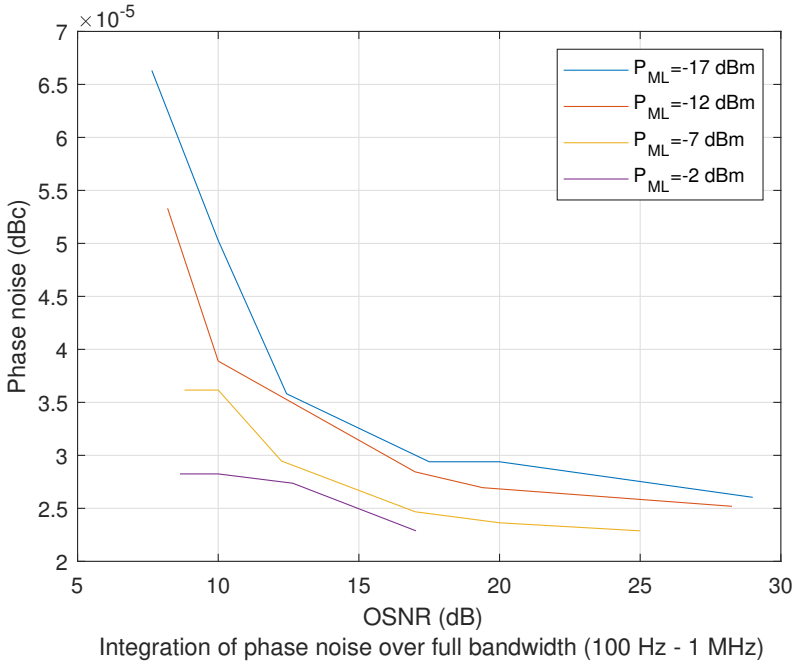

Figure 4.6: Integration of SSB phase noise spectrum for different OSNR's and ML powers

4.2 Measuring phase noise. Test 2

The aim of the second test is set a comparison with the first one by keeping OSNR constant and sweep the total power (ML and ASE noise) into the SL. For the same value of OSNR, we expect to see different phase noise, so we will be able to conclude the limiting factor of locking bandwidth (ML power solely or total power).

An OSNR of 10 dB is fixed, a sweep of P_{ML} parameter is set from 0 to -25 dBm. Figure 4.7 presents a comparison of phase noise spectrum for an OSNR of 10 dB and two different ML powers. P_{ML} = -12 dBm represents the measurement from test 1 (total power fixed), whereas P_{ML} = -10 dBm line is the test 2 measurement, where OSNR is fixed. We have to mention that ASE power is adjusted to maintain the corresponding OSNR.

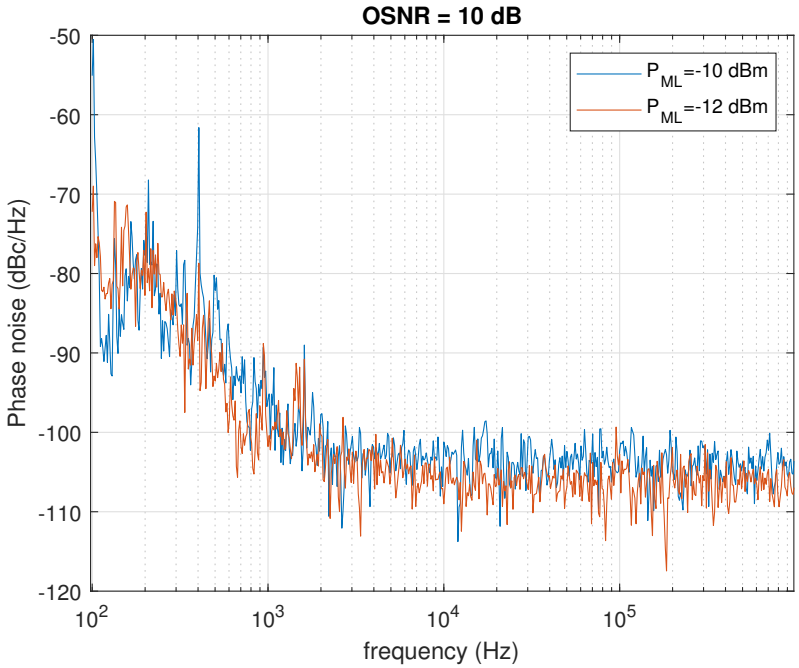

Figure 4.7: FFT of phase noise for OSNR = 10dB and setups for both tests

Even for a higher ML power locking bandwidth presents a lower value (superior phase noise) when we sweep total power. This means that locking bandwidth depends on total power injected into the slave laser, and not master power solely. If we proceed the same way than in test 1 by integrating phase noise spectrum, we will also perceive that total power limits the locking bandwidth.

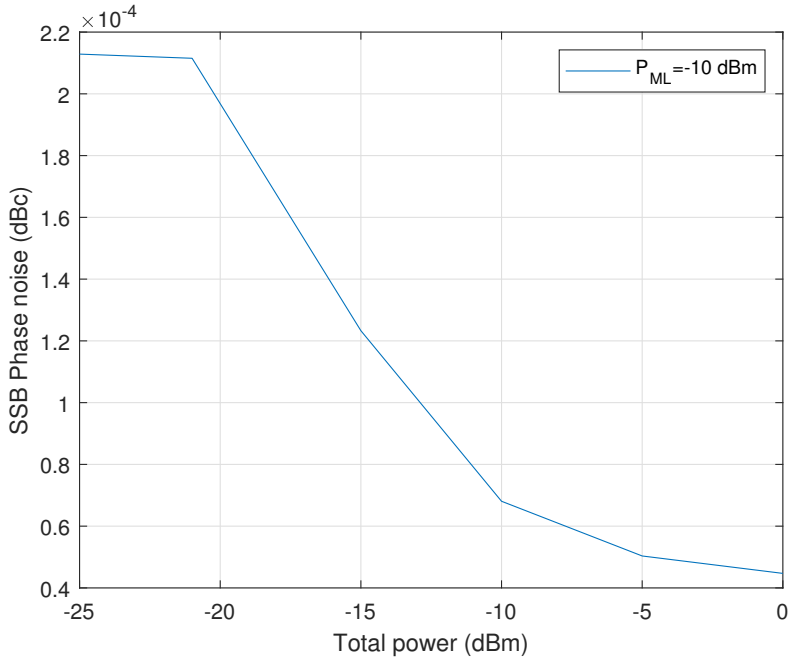

Figure 4.8: FFT of phase noise for OSNR = 10 dB and setups for both tests

Figure 4.8 shows a phase noise of 6.8x10^{-5} dBc for ML input power of -10 dBm. In graph 4.6, phase nose acquires a value below 4x10^{-5} dBc for a lower input ML power. With this test we strengthen the hypothesis that total injected power is the constraint for OIL. If there is a persistent and powerful noise source in our system, there will not be option to maintain optimal levels of locking bandwidth, regardless of how powerful ML signal is.
We also observe a linear raise of phase noise in the input power range of -10 to -20 dBm. Below this value, phase noise becomes flat, but OIL is not possible at lower ML input powers (<-25 dBm).

5
Discussion

The major finding of this work is the discovery about the main constraint in OIL. The total injected power limits the performance and not ML power itself. This is a constraint that remarks the necessity to filter or reduce all types of noise sources. In order to reduce ASE noise, it is advisable to locate band pass filters after every EDFA connected to the ML output. Otherwise, the noise figure of the system will not be enough to perform stable locking at low input powers (-45 dBm).
It is also remarkable the large difference in phase noise when P_{ML}=-23 dBm respect to the other values considered (-17 dBm,-12 dBm,...). In this case, OSNR has bigger repercussions than for others input ML powers. This is understandable due to the locking at low IR, in Eqn. (2.17), it is stated how locking bandwidth depends directly on injected power. However, if OSNR is kept high enough (26 dB), the phase noise results are similar to the ones obtained for higher ML powers. When the power at ML is greater than -17 dBm, the phase noise decrease dramatically with OSNR , so even though we confirmed locking bandwidth relayed on total power, in these cases ML is the dominating factor.
This works try to widen the knowledge about OIL, starting from the ideas presented in [1], where it is presented a procedure for OIL at a record input power of -45 dBm. With the addition of the PLL setup a limit of -55 dBm can be reached. The main advance done here is the distinction between the nature of powers into the SL. In this way, we can conclude that for every application where optical injection locking is needed, it is essential to reduce ASE noise sources and every type of losses to achieve locking at low IR. If this is not possible, amplifying the ML signal will not provide a solution to this issue. Reflections in the circulator is a factor that must be taken into account, because unwanted tones can disturb the locking mechanism.
Future lines of investigation should research on the LB limit when a PLL is working properly. Results should not show qualitative differences with conclusions made in this thesis. A PLL aims to correct phase shifts by driving the current controller of the laser. This affects the minimum power where locking is possible, improving the ML powers used in this work. Nevertheless, the same principles of functioning govern the OIL+PLL system.
To sum up, we tend to think that PLL malfunction might be caused by a wrong configuration of the PID integrator component, however the results obtained should stand for the initial setup proposed. More research could be done in order to study OIL at other wavelengths or other types of lasers. As a suggestion, studying locking range dependencies with central wavelength of ML and SL may be a way to improve current power records of OIL.

Bibliography

[1] R. Kakarla, J. Schröder, and P. Andrekson, "Optical injection locking at sub nano-watt powers," Opt. Lett. 43, 5769-5772 (2018).
[2] B. Dahmani, L. Hollberg, and R. Drullinger, "Frequency stabilization of semiconductor lasers by resonant optical feedback," Opt. Lett. 12, 876-878 (1987)
[3] Z. Ahmed, H. F. Liu, D. Novak, Y. Ogawa, M. D. Pelusi and D. Y. Kim, "Locking characteristics of a passively mode-locked monolithic DBR laser stabilized by optical injection,"IEEE Photonics Technology Letters, vol. 8, no. 1, pp. 37-39. 1996
[4] C. Chang, L. Chrostowski and C. J. Chang-Hasnain, "Injection locking of VCSELs," IEEE Journal of Selected Topics in Quantum Electronics, vol. 9, no. 5, pp. 1386-1393, 2003.
[5] A. Ryvkin, B.Panajotov, "Optical-injection-induced polarization switching in polarization-bistable vertical-cavity surface-emitting lasers," Journal of Applied Physics. 96. 6002 - 6007.
[6] T. Ramos, P. Gallion, D. Erasme, A. J. Seeds, and A. Bordonalli, "Optical injection locking and phase-lock loop combined systems," Opt. Lett. 19, 4-6 (1994).
[7] Pikovsky, A. Rosenblum, M. Kurths, (2001). Synchronization, A Universal Concept in Nonlinear Sciences. Cambridge: Cambridge University Press.
[8] R. Adler, "A Study of Locking Phenomena in Oscillators," Proceedings of the IRE, vol. 34, no. 6, pp. 351-357, 1946. doi: 10.1109/JRPROC.1946.229930
[9] Steier, W.H. Stover, H.L.. (1966). "Locking of laser oscillators by light injection", IEEE Journal of Quantum Electronics, 2. 111 - 112. 10.1109/JQE.1966.1073970.
[10] F. Mogensen, H. Olesen and G. Jacobsen, "Locking conditions and stability properties for a semiconductor laser with external light injection", IEEE Journal of Quantum Electronics, vol. 21, no. 7, pp. 784-793, 1985.
[11] G. P. Agrawal and C. M. Bowden, "Concept of linewidth enhancement factor in semiconductor lasers: its usefulness and limitations," IEEE Photonics Technology Letters, vol. 5, no. 6, pp. 640-642, 1993.
[12] https://www.rp-photonics.com/linewidthenhancementfactor.html
[13] R. Kakarla, K. Vijayan and A. Lorences, "High Sensitivity Receiver Demonstration Using Phase Sensitive Amplifier for Free-Space Optical Communication" . 1-3. 10.1109/ECOC.2017.8346152.
[14] G.Agrawal. (2012). Fiber-Optic Communication Systems: Fourth Edition. 10.1002/9780470918524.

[15] G. Agrawal, "Nonlinear fiber optics: its history and recent progress [Invited]," J. Opt. Soc. Am. B 28, A1-A10 (2011)
[16] C. Chang, L. Chrostowski and C. J. Chang-Hasnain, "Injection locking of VCSELs," IEEE Journal of Selected Topics in Quantum Electronics, vol. 9, no. 5, pp. 1386-1393, 2003.
[17] Olsson and Samuel L I. "Optical Transmission Systems Based on Phase-Sensitive Amplifiers." (2015).
[18] https://www.edmundoptics.com/resources/application-notes/optics/introduction-to-polarization/
[19] https://www.physlab.org/wp-content/uploads/2016/07/Ch6-BYUOpticsBook2013.pdf
[20] https://en.wikipedia.org/wiki/Jonescalculus
[21] R. Salem et al. "Techniques for Polarization-Independent Cross-Phase Modulation in Nonlinear Birefringent Fibers." IEEE
Journal of Selected Topics in Quantum Electronics 14 (2008): 540-550.
[22] D. Bhalla and M.Bhutani. (2014). Performance Analysis of Four Wave Mixing: A Non-Linear Effect in Optical fibers. International Journal of Computer Applications. 93. 44-49. 10.5120/16231-5720.
[23] https://www.edmundoptics.com/resources/application-notes/optics/introduction-to-polarization/
[24] https://en.wikipedia.org/wiki/Polarizer
[25] Power meter datasheet: https://img-en.fs.com/file/usermanual/fiber-optical-power-meter-fs.com.pdf
[26] Signal analyzer datasheet: https://literature.cdn.keysight.com/litweb/pdf/5989-6531EN.pdf
[27] OSA datasheet: https://accusrc.com/uploads/datasheets/5179AQ6317.pdf
[28] ESA datasheet: https://www.valuetronics.com/product/8563e-agilent-spectrum-analyzer-used
[29] Circulator datasheet: http://www.afwtechnologies.com.au/pmcirculator.html
[30] PD Datasheet: https://www.finisar.com/sites/default/files/downloads/xpdv21x0ra.pdf
[31] mixer datasheet: https://www.pasternack.com/images/ProductPDF/PE8653.pdf
[32] https://www.keysight.com/upload/cmcupload/All/PhaseNoisewebcast19Jul12.pdf

A

Appendix 1

Lorem ipsum dolor sit amet, consectetur adipisicing elit, sed do eiusmod tempor incididunt ut labore et dolore magna aliqua. Ut enim ad minim veniam, quis nostrud exercitation ullamco laboris nisi ut aliquip ex ea commodo consequat. Duis aute irure dolor in reprehenderit in voluptate velit esse cillum dolore eu fugiat nulla pariatur. Excepteur sint occaecat cupidatat non proident, sunt in culpa qui officia deserunt mollit anim id est laborum.